Emergent Materials (2019) 2:1–10
https://doi.org/10.1007/s42247-018-0020-2

ORIGINAL ARTICLE

Cooperative dynamics in a model DPPC membrane arise from membrane layer interactions

Kiley E. Kennedy[1,2] · Neha Shafique[1,3] · Jack F. Douglas[4] · Francis W. Starr[1,5]

Received: 14 August 2018 / Accepted: 19 November 2018 / Published online: 19 December 2018

Abstract

The dynamics of model membranes can be highly heterogeneous, especially in more ordered dense phases. To better understand the origins of this heterogeneity, as well as the degree to which monolayer systems mimic the dynamical properties of bilayer membranes, we use molecular simulations to contrast the dynamical behavior of a single-component dipalmitoylphosphatidylcholine (DPPC) lipid monolayer with that of a DPPC bilayer. DPPC is prevalent in both biological monolayers and bilayers, and we utilize the widely studied MARTINI model to describe the molecular interactions. As expected, our simulations confirm that the lateral structure of the monolayer and bilayer is nearly indistinguishable in both low- and high-density phases. Dynamically, the monolayer and bilayer both exhibit a drop in mobility for dense phases, but we find that there are substantial differences in the amplitude of these changes, as well as the nature of molecular displacements for these systems. Specifically, the monolayer exhibits no apparent cooperativity of the dynamics, while the bilayer shows substantial spatial and temporal heterogeneity in the dynamics. Consequently, the dynamical heterogeneity and cooperativity observed in the bilayer membrane case arises in part due to interlayer interactions. We indeed find a substantial interdigitation of the membrane leaflets which appears to impede molecular rearrangement. On the other hand, the monolayer, like the bilayer, does exhibit complex non-Brownian molecular displacements at intermediate time scales. For the monolayer system, the single particle motion can be well characterized by fractional Brownian motion, rather than being a consequence of strong correlations in the molecular motion previously observed in bilayer membranes. The significant differences in the dynamics of dense monolayers and bilayers suggest that care must be taken when making inferences about membrane dynamics on the basis of monolayer studies.

Keywords Membrane · Dynamics · Heterogeneity

Introduction

Lipid structures are one of the most ubiquitous forms of biological soft matter. Given their vital role in biological function, lipid structures, including lipid monolayers and bilayers, have been the subject of intense study for many decades [1]. Lipid bilayers form membranes that surround all cells and many sub-cellular structures and are rich in membrane proteins. Protein mobility, which is closely connected to membrane function, is highly dependent on the dynamics of the surrounding lipid matrix. While the structure and composition of lipid membranes have been studied extensively, our understanding of their dynamics is still developing [2]. Lipid monolayers form about 90% of pulmonary surfactant, a lipoprotein complex that plays a critical role in lung structure and the breathing process [3]. The absence, deficiency, or impairment of surfactant monolayers can lead to a host of medical problems, including infant respiratory distress syndrome (IRDS), which is a common disorder among premature infants. Consequently, there is widespread interest in understanding the general properties of lipid monolayers and bilayers.

Given the structural similarity between lipid monolayers and bilayers, these systems share a number of physical properties. Indeed, both systems exhibit similar structural properties across a wide range of temperatures and pressures [4], and thus share similar thermodynamic properties [5]. Both the bilayer and the monolayer also undergo a liquid-liquid phase transition from a high-density phase, which features densely packed lipids at high pressures or low temperatures,

✉ Francis W. Starr
fstarr@wesleyan.edu

Extended author information available on the last page of the article.

to a low-density phase, where lipids are more disordered at low pressures or high temperatures. In many cases, the properties of lipid monolayers are used to infer the properties of bilayers, as experiments on lipid monolayers are often easier to carry out than those on bilayers [6]. However, there are also notable differences between the monolayer and bilayer. Such distinctions are not surprising, given their functional differences: monolayers primarily act as a lubricant in the breathing process; bilayers serve as cell membranes and compartmentalize processes within cells.

While the structural and thermodynamic similarities between monolayers and membranes are documented, studies contrasting the dynamics of these lipid systems are comparatively less common. The consensus view on the nature of lipid dynamics has evolved substantially over the past several decades [1]. The fluid mosaic model [7], in which all elements undergo independent and uncorrelated lateral motion, has been supplanted on the basis of evidence for more complex correlations in lipid rearrangement [8, 9]. In particular, the concept of functional "lipid rafts" that are structurally and dynamically distinct from their surroundings [10, 11] has become a predominant view. It is widely agreed that these rafts are characterized by heterogeneous dynamics within the lipid layer that involves a combination of lipids and the protein Caveolin-1, though the quantitative description of these structures remains a broadly studied and debated topic.

Experiments and simulations on lipid layers have shown that such heterogeneity arises as a fundamental property of lipid systems [12–16], even in the absence of compositional variations. For example, neutron scattering experiments on single-component bilayers have demonstrated that lipids exhibit short-term localized mobility consistent with the formation of dynamical clusters [17], and experiments on single-component lipid monolayers observed heterogeneous rotational dynamics [18]. Simulations of pure DPPC lipid bilayers show dynamic heterogeneity in the form of lipid clusters on the size and time scales expected for lipid rafts, solely as a result of the intrinsic dynamics of the membrane lipids [15]. While peptides and proteins play a vital role in the functional heterogeneous dynamics of living membranes, it is apparent that heterogeneity can arise even without the complexity of these multiphase membranes. Accordingly, it is important to understand the underlying framework upon which these complex biomolecules must dance.

Such dynamically heterogeneous behavior is similar to that already well-established in a variety of soft condensed matter systems when the intermolecular interactions are strong relative to the thermal energy, such as occurs in simple fluids approaching a glass transition, including polymers and granular materials [19, 20]. This heterogeneity is characterized by the distinction between mesoscopic regions of varying mobility and frequently occurs without any significant change in the overall structure of these systems.

In this manuscript, we study the dynamics of simulated single-component monolayers and bilayers comprised of dipalmitoylphosphatidylcholine (DPPC) lipids to assess the degree to which the dynamics of monolayer systems mimic those of bilayer membranes, particularly with regard to cooperative lipid rearrangements. We focus on DPPC since it is the most common lipid component of pulmonary surfactant and is also prevalent in cell membranes [21]. DPPC has shown to exhibit cooperative lipid motions in single-component simulations of bilayers [13, 15], and it is one of the most frequently studied lipids [22]. While our single-component lipid structures are a substantial simplification in comparison to the multicomponent monolayers and membranes found in biological systems, these model systems allow us to explore the fundamental dynamic behavior of lipid monolayers and bilayers without the presence of multiple lipid, protein, and other membrane localized molecules (e.g., cholesterol, etc.) that complicate our understanding of the underlying mechanism responsible for dynamical heterogeneity. In our view, studying these "simple" lipid systems is a necessary early step in a bottom-up approach to comprehend the dynamics of real biological membranes; we must crawl a little before we run a marathon.

Our findings are based on molecular dynamics (MD) simulations of single-component DPPC lipid layers modeled by the coarse-grained (CG) MARTINI force field [23]. Our simulations confirm the expected similarities in the thermodynamic and structural properties of membranes and monolayers, but we find significant differences in dynamics of these lipid structures. In particular, the monolayer systems show little evidence for cooperativity of lipid displacements, unlike the behavior of lipids in membranes. Significant interdigitation of the lipid layers in membranes apparently plays an important role in the cooperativity of molecular rearrangements. These findings illustrate the potential challenges of using monolayers as model systems to describe membranes.

Model and simulations

We performed molecular dynamics simulations of DPPC monolayers and bilayers using the coarse-grained MARTINI model, which has been systematically parameterized to reproduce thermodynamic properties of lipid membranes [24]. We select DPPC because it is the most common component of surfactant monolayers and is also prevalent in cell membranes.

Our DPPC monolayer systems consist of two parallel lipid monolayers separated by a vacuum regime and a water regime, which mimics the air-water interface where

lipid monolayers are found. Periodic boundary conditions are implemented in the x-, y-, and z-directions. Each system includes a total of 2660 lipids, with 1330 lipids per monolayer. There are 66,734 CG water "molecules" separating the monolayers, and, in the MARTINI mapping, each water represents four molecules. Thus, the hydration level far exceeds the minimal amount needed to avoid effects on the dynamics [25]. The DPPC bilayer membrane simulations were reported in our earlier work [15].

All molecular dynamics simulations were performed using the GROMACS simulation suite. We use a standard integration time step 0.02 ps for the MARTINI model. Temperature and pressure were controlled by the Berendsen algorithm. We implement semi-isotropic pressure coupling, which scales the pressure in the x-y plane independently from that of the z-direction. Pressure coupling in the x-y plane is set to zero and is independent of pressure fluctuations in the z-direction, allowing us to maintain a surface tension equal to zero. Furthermore, the box in the z-direction is fixed so that the vacuum regime remains stable.

We generated initial equilibrium structures by performing 1-μs equilibration runs at temperatures between 300 and 350 K at zero surface tension. Given the propensity for hysteresis in the transition between expanded and condensed states [3], we equilibrated systems near the phase transition starting from both expanded and condensed states. Following this equilibration, "production" simulations were carried out, from which molecular coordinates were stored, and all data we shall show was collected. For systems in the liquid-expanded phase, these production runs were an additional 1 μs in duration; for the less mobile liquid-condensed phase, production runs were an additional 3 μs in duration.

Results

While lipid monolayers are interesting in their own right, monolayers are also widely studied as model systems to infer the properties of membrane systems, due to their similar properties and the ability to directly examine monolayers in a Langmuir trough. Thus, for reference, we establish the similarities in the thermodynamic and structural properties of the monolayer and membrane systems we study. We first consider the phase behavior of these systems. Both membranes and monolayers are known to exhibit a low-density, highly fluid phase, which makes a first-order phase transition to a more ordered dense phase at low temperature. However, it is important to note that the nomenclature of these phases is distinct for monolayers and bilayers: the low-density phase is referred to as the liquid-expanded (LE) state in the monolayer, while in the bilayer, this phase is called the fluid or L_α phase; the high-density phase is referred to as the liquid-condensed (LC) phase for the monolayer, while in the bilayer, this phase is called the gel or L_β phase. In the remainder of the manuscript, we often simply refer to "high-" and "low-density phases" to simplify nomenclature, regardless of whether we discuss monolayers or bilayers. Figure 1 shows mean area per lipid as a function of temperature for both systems. As expected, we see a liquid-liquid phase

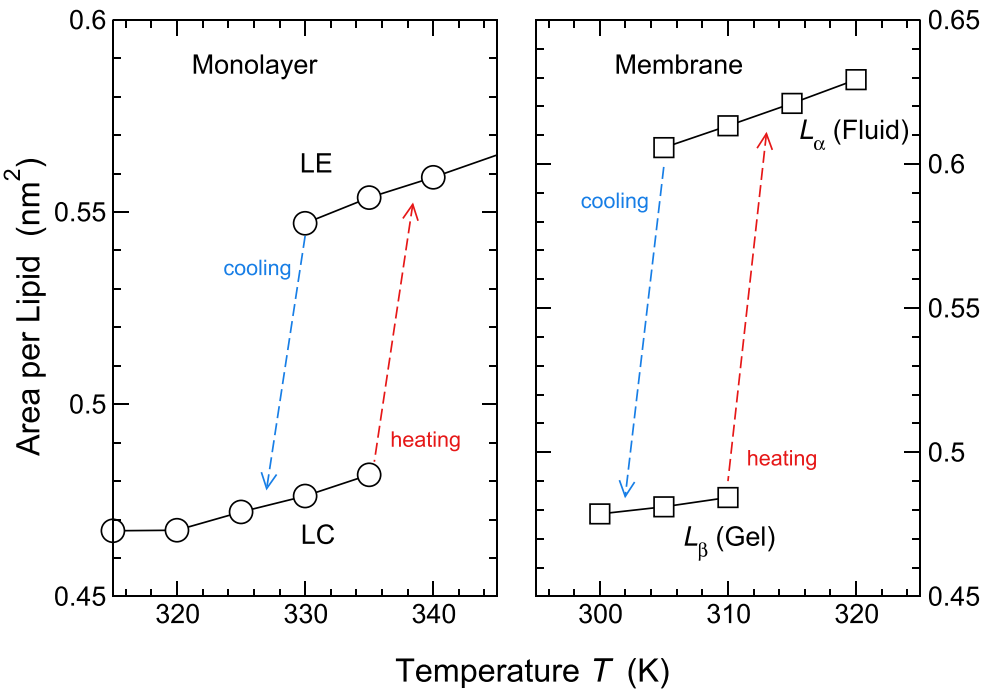

Fig. 1 **a** and **b** The area per lipid as a function of temperature shows a clear phase transition in the monolayer near 330 to 330 K and in the bilayer 305 to 310 K. The bilayer data is reproduced from previous simulation studies [15]

transition between the comparatively ordered, high-density (small area per lipid) LC/L_β phase, and the more disordered (large area per lipid) LE/L_α phase. We have driven the phase transition both by cooling the low-density phase and heating the high-density phase, and we observe modest hysteresis between the cooling and heating paths over the phase transition region. The transition region of the monolayer is at somewhat higher temperature than the experimentally observed transition of DPPC monolayers [26], similar to what was seen in earlier simulations of the MARTINI DPPC model [3].

We compare the lipid structure within a leaflet by calculating the center-of-mass structure factor

$$S(q) = \frac{1}{N}\left\langle \sum_{j,k=1}^{N} e^{i\mathbf{q}(\mathbf{r}_j - \mathbf{r}_k)} \right\rangle \quad (1)$$

where $\mathbf{r}_j$ is the position of the center-of-mass of lipid j, lipids j and k are in the same leaflet, and q is the amplitude of the scattering wave vector. $S(q)$ is related to the real--space pair correlation function $g(r)$ by a Fourier transform, and is particularly sensitive to periodicities in molecular structure. Figure 2 shows $S(q)$ in the low- and high-density phases. The low-density phase exhibits only a weak feature on the scale of the inter-lipid spacing, indicative of only weak ordering. In contrast, the high-density phase of both the monolayer and membrane shows three distinct peaks in $S(q)$ superimposed on an amorphous background. The peaks occur at approximately $q_1 = 14\ \mathrm{nm}^{-1}$, $q_2 = 24\ \mathrm{nm}^{-1}$, and $q_3 = 28\ \mathrm{nm}^{-1}$; the relationship between these three peaks is given by $q_2 \approx \sqrt{3}q_1$ and $q_3 \approx 2q_1$, suggestive of 2D hexatic ordering, an intermediate phase in 2D liquids between isotropic liquid and crystalline solid states [27]. Such ordering is well documented in prior membrane studies [14, 28–30]. In short, our simulations reaffirm the expected similarities between the thermodynamic and structure properties of the monolayer and membrane systems.

We now proceed to contrast the dynamical properties of these systems. Given the strong similarity in leaflet structure of the bilayer and monolayer, one might expect similar dynamical behavior. However, we shall show that there are significant differences in the nature of the local lipid rearrangements that we did not anticipate.

We first characterize the mean single-lipid properties in the monolayer. The in-plane mean-squared displacement (MSD) $\langle r^2(t)\rangle$ directly quantifies single-lipid dynamics and can be related to the diffusion coefficient, which is experimentally measurable. Figure 3 compares $\langle r^2(t)\rangle$ of bilayer and monolayer systems in both the low-density and high-density phases at a representative temperature; within each phase, $\langle r^2(t)\rangle$ varies only weakly with temperature, which we shall quantify when we examine the diffusion coefficient. As we expect, both the monolayer and bilayer show a considerable reduction of $\langle r^2(t)\rangle$ in the dense phase. While $\langle r^2(t)\rangle$ in the dense monolayer (LC) and bilayer (L_β) closely follow one another up to $\approx$ 50 ps, at larger times, lipids in the LC monolayer are substantially more mobile than those of the gel (L_β) membrane.

The difference in monolayer and membrane mobility can be most readily distinguished by considering the long-time

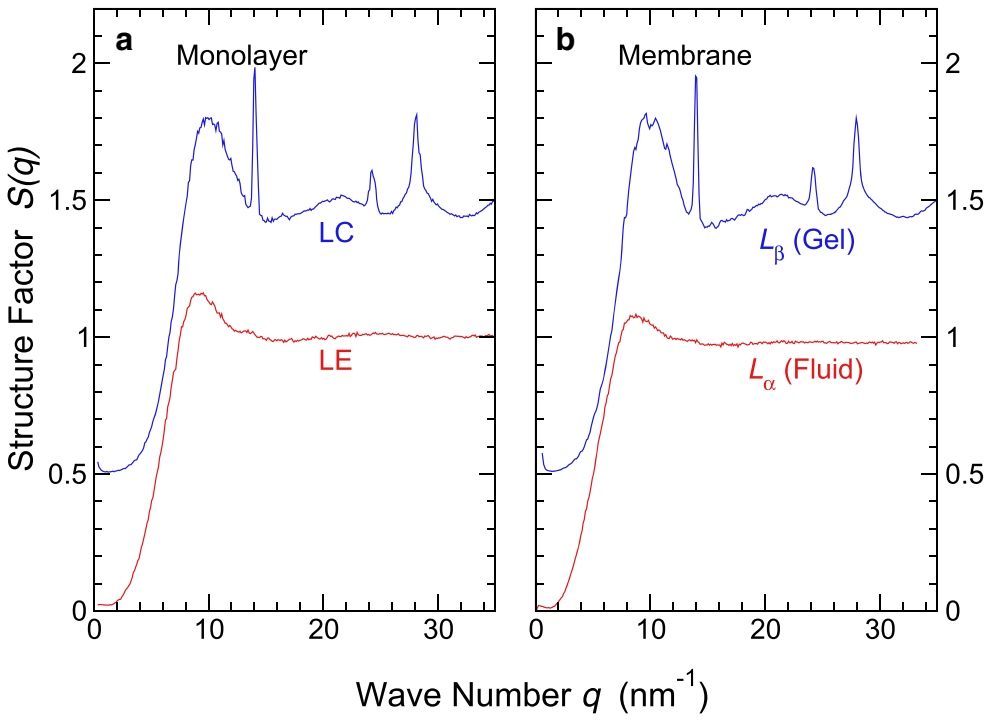

Fig. 2 The structure factor $S(q)$ of the center-of-mass of lipids in the plane of the monolayer for **a** the LC phase and **b** the LE phase. The three distinguished peaks indicate 2D hexatic ordering: for consecutive peaks $q_1 = 12\ \mathrm{nm}^{-1}$, $q_2 = 24\ \mathrm{nm}^{-1}$, and $q_3 = 28\ \mathrm{nm}^{-1}$, we find $q_2 \approx \sqrt{3}q_1$ and $q_3 \approx 2q_1$. Curves are shifted vertically for clarity. Bilayer data extracted from simulations of previous studies [15]

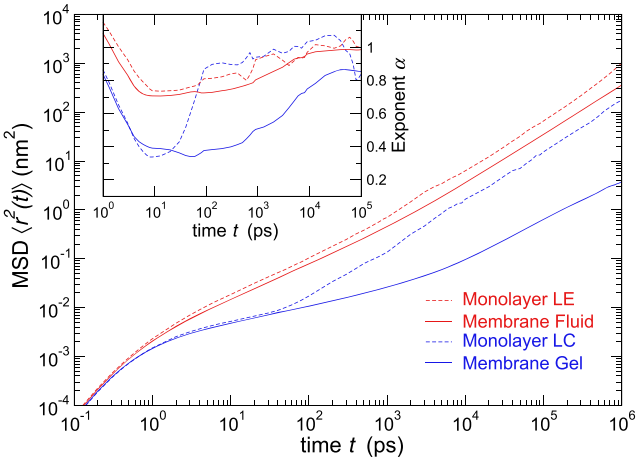

Fig. 3 A comparison of the in-plane center-of-mass $\langle r^2(t)\rangle$ for lipid monolayer and membrane systems in the low- and high-density phases. In the low-density phase, the behavior of $\langle r^2(t)\rangle$ is very similar for the monolayer in membrane. In the high-density phase, the behavior is very similar up to nearly 100 ps, but at larger times the monolayer exhibits substantially greater displacements than the membrane. The inset shows the anomalous diffusion exponent α, defined by Eq. 3. A value $\alpha < 1$ is indicative of "anomalous" diffusion

asymptotic behavior of $\langle r^2(t)\rangle$, which defines the diffusion coefficient,

$$D = \lim_{t\to\infty} \frac{\langle r^2(t)\rangle}{4t} \tag{2}$$

for motion within a plane. Figure 4 shows the diffusion coefficient D as a function of temperature for both the monolayer and membrane. While both systems show a substantial drop in D upon entering the dense phase, the bilayer gel phase has a D value roughly one order of magnitude smaller than that of the LC monolayer. Apparently, interactions between the leaflets of the bilayer substantially affect lipid mobility, a feature that has further ramifications.

In addition to simple diffusion, much attention has been given to the behavior of $\langle r^2(t)\rangle$ at intermediate times between the crossover from ballistic motion (at very short intervals) and diffusive motion (at very large intervals) [31–35]. At this intermediate time scale, $\langle r^2(t)\rangle$ exhibits sublinear growth, sometimes referred to as "anomalous diffusion." Displacements in the sub-diffusive regime can be described by $\langle r^2(t)\rangle \sim t^{\alpha}$, where α is commonly referred to as the anomalous diffusion exponent. Operationally, we can evaluate α at any time by the logarithmic derivative,

$$\alpha(t) = \frac{d\ln\langle r^2(t)\rangle}{d\ln t}. \tag{3}$$

For the phase with low density and high mobility, the inset of Fig. 3 shows that $\alpha = 0.75$ for both the monolayer and bilayer at intermediate time scales spanning less than one decade; in the phase with high density and low mobility, $\alpha \approx 0.35$ at intermediate time scales. However, the sub-diffusive power-law behavior persists for nearly two decades in the membrane, while the sub-diffusive regime in the monolayer spans no more than one decade, similar to the low-density, high-mobility phases.

This strong sub-diffusive behavior observed in the monolayer and membrane is also a characteristic feature

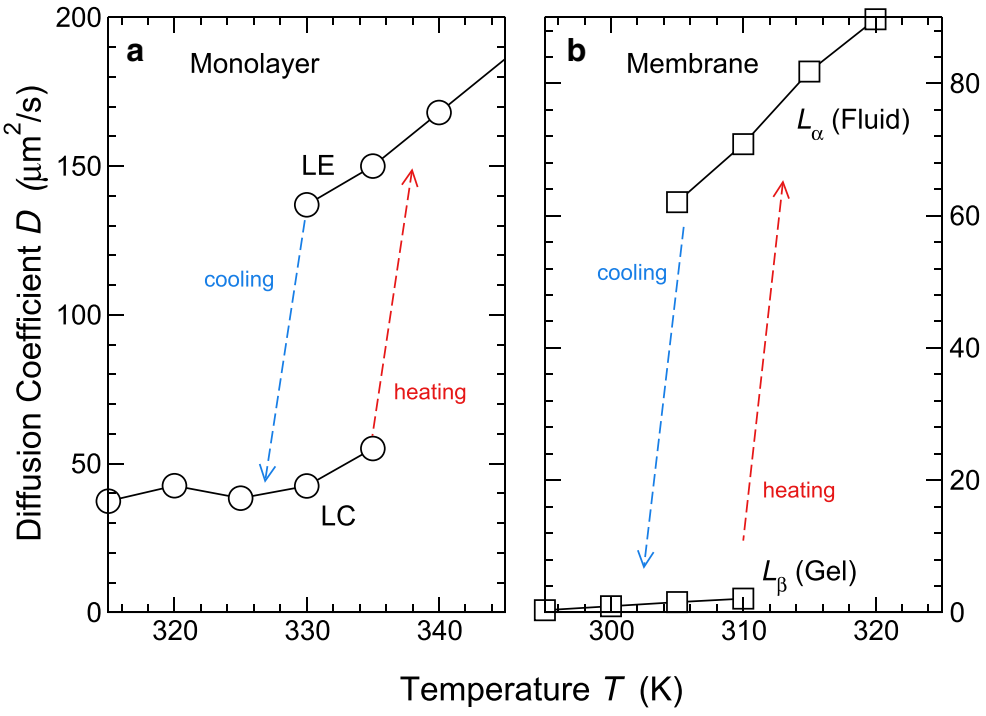

Fig. 4 **a** and **b** The diffusion coefficient D is obtained from the asymptotic behavior of $\langle r^2(t)\rangle$, and shows discontinuous drop in D on cooling to form the dense phase. Note that, in the dense phase, D for the membrane system is considerably smaller (by a factor 10) than that of the monolayer. Data for the membrane are reproduced from ref. [15]

of many glass-forming fluids [20, 36–38]. The weak dependence of $\langle r^2(t)\rangle$ on time indicates that lipids remain in a localized region close to their initial positions. This transient molecular trapping is often referred to as molecular "caging." In glass-forming systems and in our previous simulations on membrane systems [14–16], molecular caging is often associated with cooperative motion in the form of heterogeneous mesoscopic clusters of molecular units having relatively high and low mobility in comparison to ensembles of Brownian particles having the same average diffusion coefficient [38], a phenomenon referred to as "dynamical heterogeneity." We next explore the degree to which such collective molecular motion occurs in the lipid monolayer.

One common approach to quantify the degree of anomalous diffusion and molecular caging is through the (in-plane) non-Gaussian parameter,

$$\alpha_2(t) = \frac{\langle r^4(t)\rangle}{2\langle r^2(t)\rangle^2} - 1, \tag{4}$$

which compares the ratio of the second and fourth moments of the displacement. For a system obeying simple Brownian motion with Gaussian distributed displacements, $\alpha_2(t) = 0$. Note that $\alpha_2(t)$ should not be confused with the anomalous diffusion exponent α, though both provide some measure of non-Brownian molecular motion. Figure 5 compares the in-plane $\alpha_2(t)$ of monolayer and bilayer systems. As expected, all systems show that $\alpha_2(t) \approx 0$ in the ballistic regime (where displacements follow a Gaussian distribution due to the Maxwell-Boltzmann distribution of molecular speeds), as well as on the time scale for diffusive (Brownian) behavior. Moreover, $\alpha_2(t) \approx 0$ for all intermediate times in the highly mobile LE monolayer and L_α bilayer, indicating that displacements follow a simple Gaussian distribution, supporting that there is little or no dynamic heterogeneity in the form of large-scale clusters of mobile particles in the low-density phase of either the monolayer or bilayer. Our previous work [15] showed that $\alpha_2(t)$ in the high-density L_β phase of the membrane has a substantial peak at intermediate time (shown in Fig. 5), which was found to be associated with collective lipid molecule rearrangements. Given the other similarities between the monolayer and bilayer, it comes as a surprise that the dense LC monolayer exhibits *no significant peak* in $\alpha_2(t)$, and thus no significant deviations from Gaussian displacements. The close correspondance to the Gaussian model can be more clearly seen by directly comparing the distributions of lipid displacements at the time t^* of the largest value $\alpha_2(t)$, i.e., the self part of the van Hove correlation function $G_s(r, t^*)$, to the predicted Gaussian distribution based on the known mean-squared displacement. Figure 6 indeed shows that $G_s(r, t^*)$ deviates only modestly from the expected Gaussian behavior, supporting a mostly homogeneous

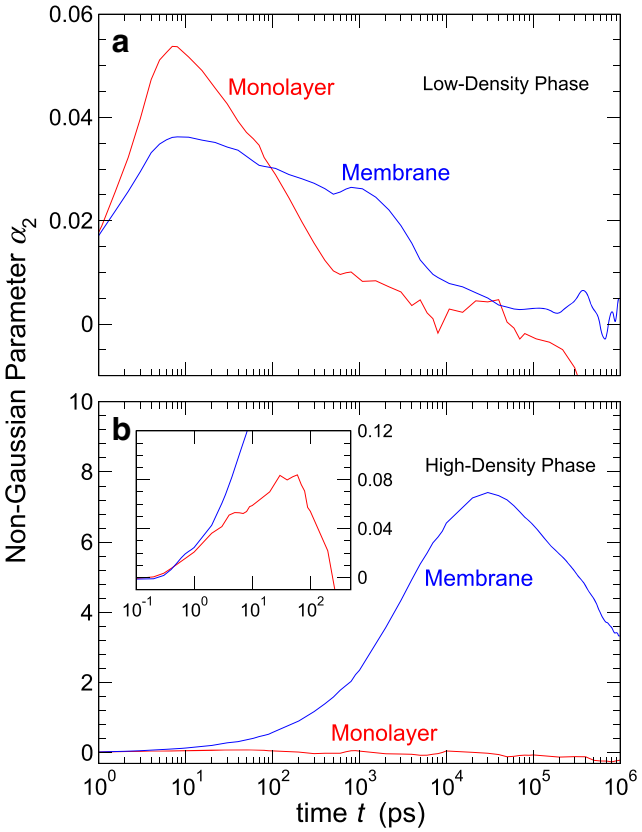

Fig. 5 The in-plane non-Gaussian parameter α_2 for the center-of-mass of lipids for **a** low-density monolayer and membrane and **b** high-density monolayer and membrane. The magnitude of the peak in α_2 provides an indication of the time scale and degree of correlated motion. In the low-density fluid phase, both the monolayer and bilayer show no indication of such dynamical correlations, as α_2 is very small fo all t. In the high-density, low-fluidity phase, the membrane shows a large peak in α_2, indicative of collective motion described in ref. [15], while the monolayer shows no indication of complex dynamics. The inset of panel (**b**) expands the vertical scale for the dense monolayer to show that α_2 has values very similar to those observed for the low-density phase in panel (**a**)

behavior of lipid motion. In contrast, significant deviations are observed for bilayers when cooperativity emerges [14–16]. The observed Gaussian behavior, coupled with anomalous power-law particle displacements $\langle r^2(t)\rangle$, are the hallmarks of Fractional Brownian motion [39–42]. Thus, the dynamics of the high-density monolayer mirrors that found in the low-density phases, albeit with a reduced overall diffusion coefficient. The analogy between the monolayer and membrane systems breaks down when we look for cooperativity of the molecular displacements in dense phases. Accordingly, there must be inter-leaflet interactions between the lipid tails that hinder simple Brownian motion, which are simply absent in the monolayer. Thus, we seek to evidence for how inter-leaflet interactions affect the cooperativity of molecular motion.

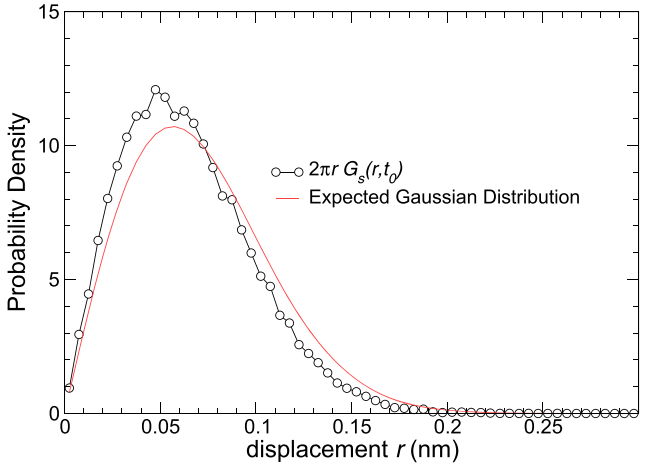

Fig. 6 The distribution of molecular displacements for the monolayer at 300 K at the time when displacements are most non-Gaussian, which defines the van Hove function $G_s(r, t^*)$. Apparently, the molecular displacements deviate only modestly from the expected from a Gaussian distribution having the same mean

The emergence of dynamical heterogeneity in the membrane (as well as other condensed phase systems) is often found to be associated with the emergence of structural ordering. Since we know that the order of the monolayer and membrane is largely the same, we first consider if differences in the head and tail group ordering might play a role. To do so, we dissect the center-of-mass $S(q)$ previously calculated into the contributions from the centers-of-mass of the head and tail groups separately, as shown in Fig. 7. In both systems, the head groups interact with water, and so no significant differences are expected, and indeed $S_{\text{head}}(q)$ for the head groups is essentially the same for the monolayer and bilayer. Unlike the overall $S(q)$, $S_{\text{head}}(q)$ does not show any characteristic sharp features, indicating that lipid head groups are disordered even in the dense phase; this should probably come as no surprise, since the head groups are considerably less bulky than the lipid tails. Hence, the sharp Bragg-like features in $S(q)$ must arise from the tail groups. Indeed, $S_{\text{tail}}(q)$ shows very sharp features at the locations previously noted for $S(q)$. Since the lipid tails in the monolayer are free, while those of the membrane layer abut the tails of the opposing layer, it is not obvious that the lateral tail structure should be the same for the monolayer and membrane. However, Fig. 7b confirms that the lateral structure for the monolayer and membrane are nearly identical, so the source of dynamical differences must have another origin.

Having established a very strong similarity in the in-plane ordering of lipids for monolayers and bilayers, the dramatic differences between the dynamics of monolayers and bilayers in the low-density phase must originate from more subtle inter-leaflet interactions. A possible explanation for the dynamical differences is that lipids from opposing leaflets interdigitate to some degree, and by doing so, further inhibit molecular rearrangement and apparently induce cooperativity in molecular motion. Such interdigitation seems unavoidable, since the bilayer is significantly less thick than twice the monolayer thickness. To quantify

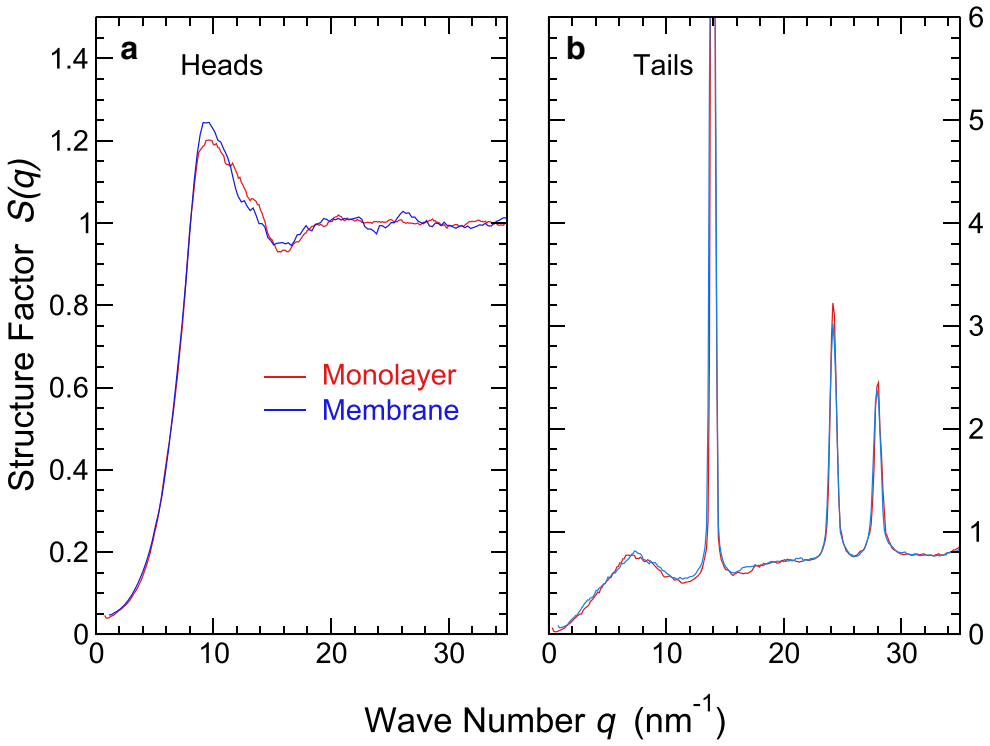

Fig. 7 Structure factor of the centers-of-mass of **a** lipid heads and **b** lipid tails. The head groups of both the LC and LE phases and the tails of the LE phase are relatively amorphous. In contrast, the LC tails exhibit crystalline ordering, which is a surprising feature given that the lipids in these systems diffuse relatively readily. Bilayer data extracted from simulations of previous studies [15]

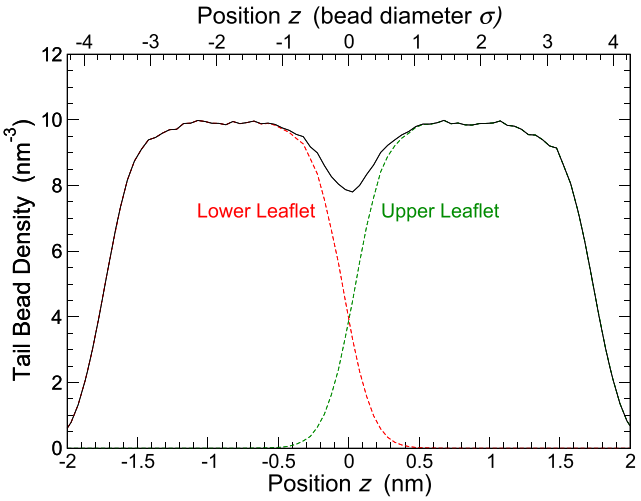

Fig. 8 The local density profile $\rho(z)$ of the tail beads of lipid bilayers for a representative $T = 305\ K$ in the gel phase. The density is evaluated over a small area 2.5 nm on an edge (containing an average of ≈ 13 lipids) to avoid a possible false signal from large-scale fluctuations in the membrane curvature. The data shows that there is substantial overlap in the ends of lipid tails in the bilayer encompassing roughly two bead diameters. Thus, lipid tails between layers substantially interdigitate

the degree to which lipid tails overlap in the dense bilayer L_β phase, we evaluate $\rho(z)$ averaged locally over small areas, roughly 2.5 nm×2.5 nm. It is important that $\rho(z)$ is examined locally, since the membrane as a whole is not flat. Figure 8 shows that the ends of lipid tails overlap substantially—over more than two bead diameters—so that the membrane features significant interdigitation of the lipid tails. Clearly, such overlaps will cause substantial correlations between lipids in opposing leaflets, which empirically results in correlations in the molecular displacements. Indeed, in an earlier study [15], we found that the islands of relative increased mobility tend to mirror each other on opposing sides of the membrane, though the result was not reported there.

Discussion and conclusion

We performed molecular dynamics simulations of lipid systems in order to contrast the dynamical behavior of lipid monolayers and bilayers and provide further insight into the origins of cooperative motions within a model DPPC bilayer membrane. Although our single-component systems are simplifications of actual biological structures, they allow us to better understand the fundamental mechanisms of cooperative lipid motions that are vital to biological function. We confirmed that lipid monolayers and bilayers exhibit very similar thermodynamic and structural organization. In this regard, the lipid monolayer can indeed be considered a helpful model to understand the properties of the bilayer membrane. However, while monolayers and bilayers exhibit similarities in their mean dynamics, such as decreased diffusivity in the high-density phase, the nature of the molecular displacements and their cooperativity is fundamentally different for monolayers and membranes: membranes exhibit spatial and temporal heterogeneity of the lipid displacements in the high-density phase, while monolayers do not. Because lipid structure within the leaflet of lipid monolayers and bilayers is nearly identical, inter-leaflet interactions in the bilayer are the origin for the observed differences between monolayers and bilayers.

A more complete understanding of the dynamics of lipid monolayers and bilayers informs experimental approaches as well as the conceptual framework upon which models of lipid dynamics are built. Our comparative study of these two lipid systems suggests that inter-leaflet interactions in membranes play an important role in the emergence of dynamical heterogeneity and, possibly, the formation of lipid rafts. Though again, we must emphasize that functional rafts depend on the interactions among the lipids, peptides, and proteins in the membrane; indeed, antimicrobial peptides such as Alamethicin can potentially disrupt raft formation [43, 44]. Experiments on lipid monolayers, which are typically easier to carry out than those on bilayers, are often used to infer properties of cell membranes; our study of the structure and dynamic behavior of these systems informs on both the strengths and limitations of this application. The substantial similarities between monolayers and bilayers in the low-density phase suggest that monolayers may be used as a model system to understand bilayers. In contrast, the dynamical behavior of high-density monolayers is qualitatively different than that of the corresponding bilayers, at least in the case of our simulated DPPC.

The next step in a comprehensive, bottom-up, approach to understanding lipid dynamics is to include other lipid types in our systems. Cholesterol is the natural choice as a second lipid component because of its prevalence in lipid monolayers and bilayers and its association with lipid raft formation in the literature [1]. Comparative studies of lipid bilayers and monolayers might reveal cholesterol's underlying role in the formation of lipid rafts. We can compare DPPC-cholesterol systems to our single-component DPPC "baseline" systems to better understand how cholesterol affects lipid clustering and heterogeneous dynamics; we can compare DPPC-cholesterol monolayers and bilayers to better understand how cholesterol flip-flopping, which leads to increased inter-leaflet interaction, might affect bilayer dynamics. Further considerations include the study of lipid monolayers at different pressures, relevant to pressure changes in surfactant monolayers.

Acknowledgements We thank C. Othon and I. Mukerji for discussions. Computer time was provided by Wesleyan University. This work was supported in part by NIST award 70NANB15H282.

References

1. L.J. Pike, J. Lipid Res. **50**(Supplement), S323 (2009)
2. K. Jacobson, O.G. Mouritsen, R.G.W. Anderson, Nat. Cell Biol. **9**(1), 7 (2007). https://doi.org/10.1038/ncb0107-7
3. S.L. Duncan, R.G. Larson, Biophys. J. **94**(8), 2965 (2008). https://doi.org/10.1529/biophysj.107.114215
4. A.K. Sum, R. Faller, J.J. de Pablo, Biophys. J. **85**(5), 2830 (2003)
5. R. MacDonald, S. Simon, Proc. Natl. Acad. Sci. **84**(12), 4089 (1987)
6. H. Brockman, Curr. Opin. Struct. Biol. **9**(4), 438 (1999)
7. S.J. Singer, G.L. Nicolson, Science **175**(4023), 720 (1972)
8. A. Lee, N. Birdsall, J. Metcalfe, P.A. Toon, G. Warren, Biochemistry **13**(18), 3699 (1974)
9. M.J. Karnovsky, A.M. Kleinfeld, R.L. Hoover, R.D. Klausner, J. Cell Biol. **94**(1), 1 (1982)
10. K. Simons, E. Ikonen, Nature **387**(6633), 569 (1997). https://doi.org/10.1038/42408
11. K. Simons, D. Toomre, Nat. Rev. Mol. Cell Biol. **1**(1), 31 (2000). https://doi.org/10.1038/35036052
12. T. Apajalahti, P. Niemelä, P.N. Govindan, M.S. Miettinen, E. Salonen, S.J. Marrink, I. Vattulainen, Faraday Discuss. **144**, 411 (2010). https://doi.org/10.1039/B901487J. http://xlink.rsc.org/?DOI=B901487J
13. E. Falck, T. Róg, M. Karttunen, I. Vattulainen, J. Am. Chem. Soc. **130**(1), 44 (2008). https://doi.org/10.1021/ja7103558
14. F.W. Starr, B. Hartmann, J.F. Douglas, Soft Matter **10**(17), 3036 (2014). https://doi.org/10.1039/C3SM53187B
15. N. Shafique, K.E. Kennedy, J.F. Douglas, F.W. Starr, J. Phys. Chem. B **120**(23), 5172 (2016). https://doi.org/10.1021/acs.jpcb.6b02982. http://fstarr.web.wesleyan.edu/publications/skds16-links.pdf. PMID: 27223339
16. Y. Oh, J. Kim, A. Yethiraj, B.J. Sung, Phys. Rev. E **93**, 012409 (2016). https://doi.org/10.1103/PhysRevE.93.012409
17. S. Busch, C. Smuda, L.C. Pardo, T. Unruh, J. Am. Chem. Soc. **132**(10), 3232 (2010). https://doi.org/10.1021/ja907581s
18. N. Dadashvand, L.A. Williams, C.M. Othon, Struct. Dyn. **1**(5), 054701 (2014)
19. J.P. Garrahan, Proc. Natl. Acad. Sci. **108**(12), 4701 (2011)
20. L. Berthier, Physics **4**, 42 (2011). https://doi.org/10.1103/Physics.4.42
21. L. Creuwels, L. Van Golde, H. Haagsman, Lung **175**(1), 1 (1997)
22. N. Kučerka, S. Tristram-Nagle, J.F. Nagle, Biophys. J. **90**(11), L83 (2015). https://doi.org/10.1529/biophysj.106.086017. http://www.cell.com/biophysj/abstract/S0006-3495(06)72564-4
23. S. Marrink. MARTINI: biomolecular forcefield for coarse grained simulations. http://md.chem.rug.nl/marrink/coarsegrain.html
24. S.J. Marrink, H.J. Risselada, S. Yefimov, D.P. Tieleman, A.H. de Vries, J. Phys. Chem. B **111**(27), 7812 (2007). https://doi.org/10.1021/jp071097f
25. M. Lis, A. Wizert, M. Przybylo, M. Langner, J. Swiatek, P. Jungwirth, L. Cwiklik, Phys. Chem. Chem. Phys. **13**(39), 17555 (2011)
26. J.M. Crane, G. Putz, S.B. Hall, Biophys. J. **77**(6), 3134 (1999). https://doi.org/10.1016/S0006-3495(99)77143-2. http://www.sciencedirect.com/science/article/pii/S0006349599771432
27. E.P. Bernard, W. Krauth, Phys. Rev. Lett. **107**, 155704 (2011). https://doi.org/10.1103/PhysRevLett.107.155704
28. G.S. Smith, E.B. Sirota, C.R. Safinya, R.J. Plano, N.A. Clark, J. Chem. Phys. **92**(7), 4519 (1990)
29. S.J. Marrink, J. Risselada, A.E. Mark, hem. Phys. Lipids **135**(2), 223 (2005). https://doi.org/10.1016/j.chemphyslip.2005.03.001
30. S.L. Duncan, I.S. Dalal, R.G. Larson, Biochimica et Biophysica Acta (BBA) - Biomembranes **1808**(10), 2450 (2011). https://doi.org/10.1016/j.bbamem.2011.06.026. http://www.sciencedirect.com/science/article/pii/S0005273611002045
31. J.H. Jeon, H.M.S. Monne, M. Javanainen, R. Metzler, Phys. Rev. Lett. **109**(18), 188103 (2012). https://doi.org/10.1103/PhysRevLett.109.188103. http://www.ncbi.nlm.nih.gov/pubmed/23215336
32. J. Ehrig, E.P. Petrov, P. Schwille, Biophys. J. **100**(1), 80 (2011). https://doi.org/10.1016/j.bpj.2010.11.002. http://www.sciencedirect.com/science/article/pii/S0006349510013688
33. M. Javanainen, H. Hammaren, L. Monticelli, J.H. Jeon, M.S. Miettinen, H. Martinez-Seara, R. Metzler, I. Vattulainen, Faraday Discuss. **161**, 397 (2013). https://doi.org/10.1039/C2FD20085F. http://pubs.rsc.org/en/content/articlehtml/2013/fd/c2fd20085f
34. P.S. Niemelä, M.S. Miettinen, L. Monticelli, H. Hammaren, P. Bjelkmar, T. Murtola, E. Lindahl, I. Vattulainen, J. Am. Chem. Soc. **132**(22), 7574 (2010). https://doi.org/10.1021/ja101481b
35. G.R. Kneller, K. Baczynski, M. Pasenkiewicz-Gierula, J. Chem. Phys. **135**(14), 141105 (2011). https://doi.org/10.1063/1.3651800. http://www.ncbi.nlm.nih.gov/pubmed/22010688
36. M.D. Ediger, Annu. Rev. Phys. Chem. **51**(1), 99 (2000). https://doi.org/10.1146/annurev.physchem.51.1.99
37. R. Richert. J. Phys. Condens. Matter **14**(23), R703 (2002). http://stacks.iop.org/0953-8984/14/i=23/a=201
38. F.W. Starr, J.F. Douglas, S. Sastry, J. Chem. Phys. **138**(12), 12A541 (2013). https://doi.org/10.1063/1.4790138. http://link.aip.org/link/?JCP/138/12A541/1
39. S. Saw, N.L. Ellegaard, W. Kob, S. Sastry, Phys. Rev. Lett. **103**, 248305 (2009). https://doi.org/10.1103/PhysRevLett.103.248305
40. S.C. Lim, S.V. Muniandy, Phys. Rev. E **66**, 021114 (2002). https://doi.org/10.1103/PhysRevE.66.021114
41. R. Ramshankar, D. Berlin, J.P. Gollub, Physics of Fluids A: Fluid Dynamics **2**(11), 1955 (1990). https://doi.org/10.1063/1.857671
42. K.L. Sebastian, J. Phys. A Math. Gen. **28**(15), 4305 (1995). http://stacks.iop.org/0305-4470/28/i=15/a=011
43. D. Constantin, G. Brotons, A. Jarre, C. Li, T. Salditt, Biophys. J. **92**(11), 3978 (2007). https://doi.org/10.1529/biophysj.106.101204. http://www.sciencedirect.com/science/article/pii/S0006349507711979
44. F. Domenici, F. Dell'Unto, D. Triggiani, C. Olmati, C. Castellano, F. Bordi, A. Tiezzi, A. Congiu, Biochim. Biophys. Acta **1850**(4), 759–768 (2015). https://doi.org/10.1016/j.bbagen.2015.01.006

Affiliations

Kiley E. Kennedy[1,2] · Neha Shafique[1,3] · Jack F. Douglas[4] · Francis W. Starr[1,5]

Kiley E. Kennedy
kk3107@columbia.edu

Neha Shafique
Neha_Shafique@hms.harvard.edu

Jack F. Douglas
jack.douglas@nist.gov

1 Department of Physics, Wesleyan University, Middletown, CT 06459, USA

2 Physics Department, Columbia University, New York, NY 10027, USA

3 Harvard Medical School, Boston, MA 02115, USA

4 Materials Science and Engineering Division, National Institute of Standards and Technology, Gaithersburg, MD 20899, USA

5 Department Molecular Biology & Biochemistry, Wesleyan University, Middletown, CT 06459, USA